A Study on Assessment of Composite Couplings for Helicopter Rotor Blades with Multi-cell Sections

Sung Nam Jung*, Il-ju Park and Eui Sup Shin*****
Chonbuk National University, Chonju 561-756, South Korea

Inderjit Chopra****
University of Maryland, College Park, MD 20742, USA

Abstract

In this work, a closed-form analysis is performed for the structural response of coupled composite blades with multi-cell sections. The analytical model includes the effects of shell wall thickness, transverse shear, torsion warping and constrained warping. The mixed beam approach based on Reissner's semi-complementary energy functional is used to derive the beam force-displacement relations. The theory is validated against experimental test data and other analytical results for coupled composite beams and blades with single-cell box-sections and two-cell airfoils. Correlation of the present method with experimental results and detailed finite element results is found to be very good.

Key Word : coupled composite blades, multi-cell sections, mixed beam approach, transverse shear, warping

Introduction

There have been a few selected research activities to model and analyze composite beams and blades with multi-cell sections. Mansfield[1] developed a flexibility formulation for thin-walled composite beams with two-cell cylindrical tube section. The equilibrium equations of shell wall were used to derive the (4×4) flexibility matrix that captures the classical four beam variables (extension, bendings in two planes, and torsion). Volovoi and Hodges[2] used the variational asymptotic approach to derive the asymptotically correct (4×4) stiffness matrix for thin-walled anisotropic beams with single- and double-celled box sections. Numerical results were presented to show the importance of incorporating shell bending strain measures even for closed thin-walled cross sections in the beam formulation. They presented results indicating that published analytical theories (e.g., Badir[3]) did not take into account the influence of shell bending strain measures correctly. Chandra and Chopra[4] investigated both analytically and experimentally the structural response of two-cell composite blades with extension-torsion couplings. The stiffness matrix derived was of the order of (9×9) since they include derivatives of shear strains as independent variables in order to include transverse shear couplings in their formulation.

Recently, Jung, et al[5]. developed a mixed beam theory that takes into account the effects

* Associate Professor, RCIT, Engineering Research Institute
E-mail : snjung@moak.chonbuk.ac.kr, TEL : 063-270-2469, FAX : 063-270-2472
** Graduate Student, Department of Aerospace Engineering
*** Full-time Lecturer, Department of Aerospace Engineering
**** Professor. Alfred Gessow Rotorcraft Center

of elastic couplings, transverse shear deformation, warping, warping restraint, and bending and shear of the shell wall. The resulting (7×7) stiffness matrix characterizes elastic properties of the beam in terms of the axial, flap and lag bending, flap and lag shear, torsion, and torsion-warping deformations. The theory was applied to open and closed (single-cell) cross-section beams and a good correlation was achieved in comparison with experimental test data.

In the present work, the mixed formulation developed in Ref. 5 has been applied to analyze coupled composite beams and blades with single-cell box sections and two-cell airfoil. The formulation is validated by comparison of the values of cross-sectional properties and steady response of multi-celled section blades with experimental results and also those from existing analysis methods found in the literature.

Compared with Volovoi and Hodges[2], the present analysis has additional features in that: (1) the influence of the thickness of shell wall with shear deformation (Reissner-Mindlin) effects are incorporated; (2) analytical expressions of Timoshenko shear correction factors are derived; (3) no asymptotic arguments to delete any terms are employed in the current framework of the analysis.

Formulation

Figure 1a shows the geometry and generalized forces for a composite blade with an arbitrary cross-section. Two systems of coordinate axes are used: an orthogonal Cartesian coordinate system (x, y, z) for the blade, where x is the reference axis of the blade and y and z are the transverse coordinates of the cross section; a curvilinear coordinate system (x, s, n) for the shell wall of the section, where s is a contour coordinate measured along the middle surface of the shell wall and n is normal to this contour coordinate. Figure 1b shows the stress resultants, moment resultants and transverse shear forces acting on a general shell segment of the blade.

The global deformations of the beam are (U, V, W) along the x, y and z axes, and ϕ is the twist about the x-axis. The local shell deformations are (u, v_t, v_n) along the x, s and n directions, respectively.

Following Ref. 5, the strain-displacement relation of the shell wall can be written as:

$$\begin{aligned}
\varepsilon_{xx} &= U_{,x} + z\beta_{y,x} + y\beta_{z,x} - \bar{\omega}\phi_{,xx} \\
\gamma_{xs} &= \gamma_{xy}y_{,s} + \gamma_{xz}z_{,s} = u^0_{,s} + V_{,x}y_{,s} + W_{,x}z_{,s} + r\phi_{,x} \\
\kappa_{xx} &= \beta_{z,x}z_{,s} - \beta_{y,x}y_{,s} + q\phi_{,xx} \\
\kappa_{xs} &= 2\phi_{,x} + \frac{1}{a}(\beta_z y_{,s} + \beta_y z_{,s} - r\phi_{,x}) \\
\gamma_{xn} &= u^0_{,n} + V_{,x}z_{,s} - W_{,x}y_{,s} - q\phi_{,x}
\end{aligned} \tag{1}$$

where a is the local shell radius of curvature and $\bar{\omega}$ is the sectorial area which is defined as:

$$\bar{\omega} = \int_0^s r\,ds \tag{2}$$

Assuming the hoop stress flow N_{ss} is negligibly small, the constitutive relations for the shell wall of the section are obtained as [5]

$$\begin{Bmatrix} N_{xx} \\ N_{xs} \\ M_{xx} \\ M_{ss} \\ M_{xs} \end{Bmatrix} = \begin{bmatrix} A'_{11} & A'_{16} & B'_{11} & B'_{12} & B'_{16} \\ A'_{16} & A'_{66} & B'_{16} & B'_{26} & B'_{66} \\ B'_{11} & B'_{16} & D'_{11} & D'_{12} & D'_{16} \\ B'_{12} & B'_{26} & D'_{12} & D'_{22} & D'_{26} \\ B'_{16} & B'_{66} & D'_{16} & D'_{26} & D'_{66} \end{bmatrix} \begin{Bmatrix} \varepsilon_{xx} \\ \gamma_{xs} \\ \kappa_{xx} \\ \kappa_{ss} \\ \kappa_{xs} \end{Bmatrix} \tag{3}$$

where the primes over the stiffness constants indicate that these are reconstructed using the zero hoop flow assumption ($N_{ss}=0$) from the original A_{ij}, B_{ij} and D_{ij} coefficients of the Classical Lamination Theory. In the present approach, we treat the strain measures $\varepsilon_{xx}, \kappa_{xx}$ and κ_{xs} as the

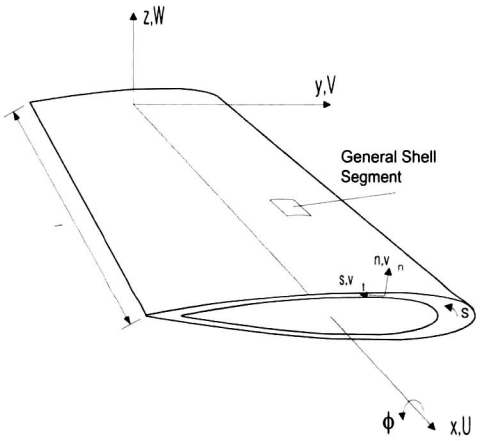

Fig. 1a. Geometry and coordinate systems.

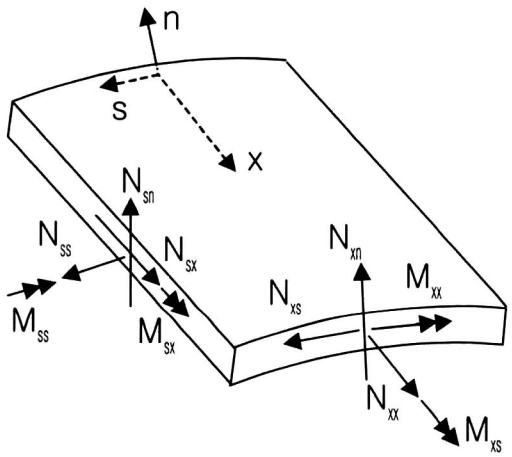

Fig. 1b. Shell forces and moments.

known and derive expressions for the shear flow N_{xs} and the hoop moment M_{ss} in terms of these quantities using the equilibrium equations of the shell wall. It is convenient to write Eq. (3) in a semi-inverted form as:

$$\begin{Bmatrix} N_{xx} \\ M_{xx} \\ M_{xs} \\ \gamma_{xs} \\ \kappa_{ss} \end{Bmatrix} = \begin{bmatrix} C_{n\varepsilon} & C_{n\kappa} & C_{n\phi} & C_{n\gamma} & C_{n\tau} \\ C_{n\kappa} & C_{m\kappa} & C_{m\phi} & C_{m\gamma} & C_{m\tau} \\ C_{n\phi} & C_{m\phi} & C_{\phi\phi} & C_{\phi\gamma} & C_{\phi\tau} \\ -C_{n\gamma} & -C_{m\gamma} & -C_{\phi\gamma} & C_{\gamma\gamma} & C_{\gamma\tau} \\ -C_{n\tau} & -C_{m\tau} & -C_{\phi\tau} & C_{\gamma\tau} & C_{\tau\tau} \end{bmatrix} \begin{Bmatrix} \varepsilon_{xx} \\ \kappa_{xx} \\ \kappa_{xs} \\ N_{xs} \\ N_{ss} \end{Bmatrix} \tag{4}$$

or in symbolic notation

$$\{s\} = [C]\{e\} \tag{4a}$$

In order to assess the semi-inverted constitutive relations (4) into the beam formulation, a modified form of Reissner's semi-complimentary energy functional Φ_R is introduced:

$$\Phi_R = \frac{1}{2}[N_{xx}\varepsilon_{xx} + M_{xx}\kappa_{xx} + M_{xs}\kappa_{xs} - N_{xs}\gamma_{xs} - M_{ss}\kappa_{ss}] \tag{5}$$

The stiffness matrix relating beam forces to beam displacements is obtained by using the variational statement of the Reissner's functional which is given by

$$\delta \int_0^l \int_C \left\{ [\Phi_R + \gamma_{xs}N_{xs} + \kappa_{ss}M_{ss}] + \left[\frac{1}{2} N_{xs}(\gamma_{xs} - u_{,s} - v_{t,x})\right] \right\} dsdx = 0 \tag{6}$$

where l is the length of the blade. In Eq. (6), the first bracketed terms are the strain energy density of the blade and the second one is the constraint condition with N_{xs} acting as the Lagrange multiplier. Performing the integrals, Eq. (6) results in the equilibrium equations of an element of the shell wall as well as the constraint conditions, which are found as:

$$\begin{aligned} &N_{xx,x} + N_{xs,s} = 0 \\ &N_{xs,x} = 0 \\ &M_{xx,x} + M_{xs,s} = 0 \\ &M_{xs,x} + M_{ss,s} = 0 \\ &\gamma_{xs} - u^0_{,s} - v_{t,x} = 0 \\ &\kappa_{ss} - \phi_{s,s} = 0 \end{aligned} \tag{7}$$

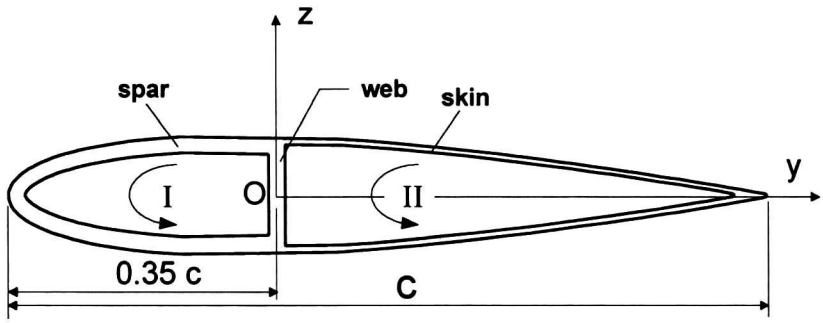

Fig. 2. Schematic of a two-cell airfoil section.

The first two equations in Eq. (7) indicate that N_{xs} consists of a constant part and a part that depends on the s-integral of $N_{xx,x}$. In addition, it is found from the third and fourth equations in Eq. (7) that M_{ss} has a constant part, a part that varies linearly with s and a part that depends on the s-integral of $M_{xs,x}$. Hence, one can write

$$\begin{aligned} N_{xs} &= N_{xs}^0 - \int_0^s (A_{11}' \epsilon_{xx,x} + B_{16}' \kappa_{xs,x}) ds \\ M_{ss} &= M_{ss}^0 + y M_{ss}^y + z M_{ss}^z - \int_0^s (B_{16}' \epsilon_{xx,x} + D_{16}' \kappa_{xs,x}) ds \end{aligned} \tag{8}$$

where $N_{xs}^0, M_{ss}^0, M_{ss}^y, M_{ss}^z$ represent the circuit shear flows for each cell of a closed multi-cell section[6]. For a two-cell blade, these lead to eight unknowns which are expressed as:

$$\{n\} = \lfloor n_1 \;\; n_2 \;\; m_1 \;\; m_2 \;\; m_1^y \;\; m_2^y \;\; m_1^z \;\; m_2^z \rfloor^T \tag{9}$$

The continuity condition that must be satisfied for each wall of the section yields the following set of equations

$$\begin{aligned} &\oint_I \gamma_{xs} ds = 2A_1 \phi_{,x}, && \oint_{II} \gamma_{xs} ds = 2A_2 \phi_{,x} \\ &\oint_I \kappa_{ss} ds = 0, && \oint_{II} \kappa_{ss} ds = 0 \\ &\oint_I y \kappa_{ss} ds = 0, && \oint_{II} y \kappa_{ss} ds = 0 \\ &\oint_I z \kappa_{ss} ds = 0, && \oint_{II} z \kappa_{ss} ds = 0 \end{aligned} \tag{10}$$

where the subscripts I and II indicate integration over the contour of cells I and II, respectively (see Fig. 2). Inserting Eq. (4) into Eq. (10), the unknowns shear flows can be obtained as

$$\begin{aligned} \{n\} &= [Q]^{-1} \cdot \left([P] \{ \bar{q}_b \} + [R] \{ \bar{q}_{b,x} \} \right) \\ &= [b] \{ \bar{q}_b \} + [B] \{ \bar{q}_{b,x} \} \end{aligned} \tag{11}$$

where

$$\{ \bar{q}_b \} = \lfloor U_{,x} \;\; \beta_{y,x} \;\; \beta_{z,x} \;\; \phi_{,x} \;\; \phi_{,xx} \rfloor^T \tag{12}$$

In Eq. (11), $[Q]$ is a symmetric (8×8) matrix and $[P]$ is a (8×5) matrix. Note that these matrices are integrals over the contour. Using Eq. (11), the shear flow and the hoop moment, Eq (8), can be expressed as

$$\begin{Bmatrix} N_{xs} \\ M_{ss} \end{Bmatrix} \equiv \{\xi\} = \{\xi^a\} + \{\xi^r\} = [f] \{ \bar{q}_b \} + [F] \{ \bar{q}_{b,x} \} \tag{13}$$

It is noted that N_{xs} and M_{ss} should be determined separately for each cell. The shear flow components N_{xs} and M_{ss} are composed of an active and a reactive part according to the terminology introduced in Gjelsvik[6]. The superscripts a and r appeared in Eq. (13) reflect this aspect.

Equation (6) can be rewritten by use of Eq. (4a),

$$\delta\int_0^l\int_c\frac{1}{2}[\{e_1\}^T[C]\{e_1\}+2\{\xi^a\}^T[\Lambda]\{\xi^r\}+\{\xi^r\}^T[\Lambda]\{\xi^r\}+N_{xs}(\gamma_{xs}-u_{,s}-v_{t,x})]dsdx=0 \tag{14}$$

where

$$\begin{aligned}\{e_1\} &= \lfloor\ \varepsilon_{xx}\ \kappa_{xx}\ \kappa_{xs}\ N_{xs}^a\ M_{ss}^a\ \rfloor^T\\ [\Lambda] &= \begin{bmatrix} C_{rr} & C_{rt}\\ C_{rt} & C_{tt}\end{bmatrix}\end{aligned} \tag{15}$$

The first term in Eq. (14) can be written in terms of beam displacements by using Eqs. (1) and (13),

$$\delta\int_0^l\int_c\frac{1}{2}\{\bar{q}_b\}^T[T]^T[C][T]\{\bar{q}_b\}dsdx=\delta\int_0^l\frac{1}{2}\{\bar{q}_b\}^T[\hat{K}_{bb}]\{\bar{q}_b\}dx \tag{16}$$

where

$$[T]=\begin{bmatrix}1 & z & y & 0 & -\bar{\omega}\\ 0 & -y_{,s} & z_{,s} & 0 & q\\ 0 & 0 & 0 & 2 & 0\\ f_x & f_y & f_z & f_\phi & f_\omega\\ g_x & g_y & g_z & g_\phi & g_\omega\end{bmatrix} \tag{17}$$

The cross-section stiffness matrix $[\hat{K}_{bb}]$ in Eq. (16) relates the cross-section force and moment resultants with beam displacements in an Euler-Bernoulli level of approximation and is given by:

$$\{\bar{F}_b\}=\lfloor\ N\ M_y\ M_z\ T\ M_\omega\ \rfloor^T=[\hat{K}_{bb}]\{\bar{q}_b\} \tag{18}$$

where N is the axial force, M_y and M_z are bending moments about y and z directions, respectively, T is the twisting moment and M_ω is the Vlasov bi-moment. In order to obtain the equivalent of a Timoshenko theory for the blade, we consider a cantilevered blade loaded at the tip with shear forces V_y and V_z. Differentiating Eq. (18) with respect to x, we obtain

$$\{\bar{F}_{b,x}\}=\lfloor\ 0\ V_z\ V_y\ 0\ 0\ \rfloor^T=[\hat{K}_{bb}]\{\bar{q}_{b,x}\} \tag{19}$$

considering Eqs. (13) and (19), one can obtain the reactive part of the shear flows $\{\xi^r\}$ as

$$\begin{aligned}\{\xi^r\} &= [F][\hat{K}_{bb}]^{-1}\{\bar{F}_{b,x}\}\\ &= \begin{bmatrix} f_y^r & f_z^r\\ g_y^r & g_z^r\end{bmatrix}\begin{Bmatrix}V_y\\ V_z\end{Bmatrix}\equiv[f^r]\{\bar{v}_s\}\end{aligned} \tag{20}$$

Combining this result with Eq. (16), Eq. (14) yields the following equation:

$$\delta\frac{1}{2}\int_0^l\lfloor\ \bar{q}_b\ \bar{v}_s\ \rfloor\begin{bmatrix}\hat{K}_{bb} & \hat{K}_{bv}\\ \hat{K}_{bv}^T & \hat{K}_{vv}\end{bmatrix}\begin{Bmatrix}\bar{q}_b\\ \bar{v}_s\end{Bmatrix}dx+\delta\frac{1}{2}\int_0^l\oint N_{xs}(\gamma_{xs}-u_{,s}-v_{t,x})dsdx=0 \tag{21}$$

where

$$\begin{aligned}\lfloor\ \hat{K}_{bv}\ \rfloor &= [f]^T[\Lambda]\lfloor\ f^r\ \rfloor\\ \lfloor\ \hat{K}_{vv}\ \rfloor &= [f^r]^T[\Lambda]\lfloor\ f^r\ \rfloor\end{aligned} \tag{22}$$

V_y and V_z are determined such that Eq. (21) is satisfied. Inserting Eqs. (1) and (4) into the second part of Eq. (21), the shear forces $\{\bar{v}_s\}$ can be related with beam displacement vector $\{q\}$ as:

$$\{\bar{v}_s\}=[p]\{q\} \tag{23}$$

where

$$\{q\}=\lfloor\ U_{,x}\ \beta_{y,x}\ \beta_{z,x}\ \phi_{,x}\ \phi_{,xx}\ \gamma_{xy}\ \gamma_{xz}\ \rfloor^T \tag{24}$$

The elements of the (2×7) matrix $[p]$ in Eq. (23) are the same as those obtained using the first

order shear deformation theory with shear correction factors of unity. By comparing Eq. (21) and Eq. (23) we get:

$$\begin{Bmatrix} \bar{q}_b \\ \bar{v}_s \end{Bmatrix} = \begin{bmatrix} [I_{5\times5}] & [0_{5\times2}] \\ [p_1] & [p_2] \end{bmatrix} \{q\} \tag{25}$$

where $[I_{5\times5}]$ is a (5×5) identity matrix and $[0_{5\times2}]$ is a null matrix of size (5×2), while $[p_1]$ has a size of (2×5) and $[p_2]$ has a dimension of [2×2]. Using Eq. (25), the first part of Eq. (21) yields the following equation:

$$\int_0^l \lfloor \delta \bar{q}_b \;\; \delta \bar{v}_s \rfloor \begin{bmatrix} \hat{K}_{bb} & \hat{K}_{bv} \\ \hat{K}_{bv}^T & \hat{K}_{vv} \end{bmatrix} \begin{Bmatrix} \bar{q}_b \\ \bar{v}_s \end{Bmatrix} dx = \int_0^l \{\delta q\}^T [K] \{q\} dx \tag{26}$$

where the (7×7) stiffness matrix $[K]$ is given by

$$\begin{aligned} [K] &= \begin{bmatrix} K_{bb} & K_{bv} \\ K_{bv} & K_{vv} \end{bmatrix} \\ &= \begin{bmatrix} \{\hat{K}_{bb} + 2\hat{K}_{bv}p_1 + p_1^T \hat{K}_{vv} p_1\} & \{\hat{K}_{bv}p_2 + p_1^T \hat{K}_{vv} p_2\} \\ \{\hat{K}_{bv}p_2 + p_1^T \hat{K}_{vv} p_2\} & \{p_2^T \hat{K}_{vv} p_2\} \end{bmatrix} \end{aligned} \tag{27}$$

The stiffness matrix $[K]$ in Eq. (27) represents the idealization of the blade at a Timoshenko level for bending and shear, while the torsion is idealized as the Vlasov torsion. Note that the (5×5) stiffness matrix $[K_{bb}]$ is modified by the shear related terms.

Results and Discussions

Numerical investigation has been performed to correlate the current analysis with available literature. The examples include single-cell box-section beams with extension-torsion or bending-torsion couplings and two-cell composite blades with bending-torsion couplings.

Single-cell Composite Box-Beam

The first example presented is single-celled, thin-walled composite box-beams with bending-torsion or extension-torsion couplings. Four different cases are considered. Fig. 3 shows the configuration details of the box sections. Each wall of the box section is composed of $[\theta_3/-\theta_3]$ or $[-\theta_3/\theta_3]$ such that extension-torsion (cases 1 and 2) or bending-torsion (cases 3 and 4) couplings are obtained. Note that Case 2 is of circumferentially uniform stiffness construction while the others present circumferentially asymmetric but alternating stiffness values. The geometry and material properties are summarized in Table 1.

As can be inferred from the layups shown in Fig. 3, there exists an important coupling B_{26} between

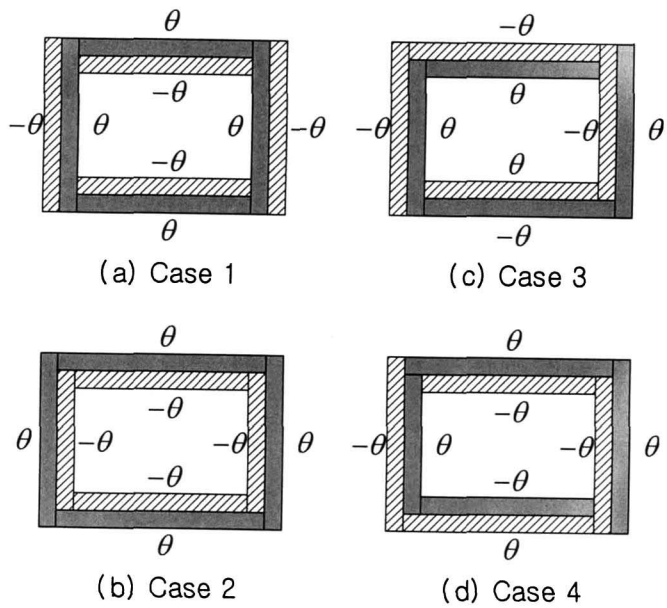

Fig. 3. Lay-up cases of box-beams.

Table 1. Geometry and material properties of graphite-epoxy box-beams

Properties	Values
E_{11}	141.9GPa
E_{22}	9.78GPa
G_{12}	6.13GPa
ν_{12}	0.42
ρ	1449kg/m^3
Ply thickness, *tp*	0.127mm
Outer width, *2b*	24.21mm
Outer height, *2h*	13.64mm
Length, *l*	762mm

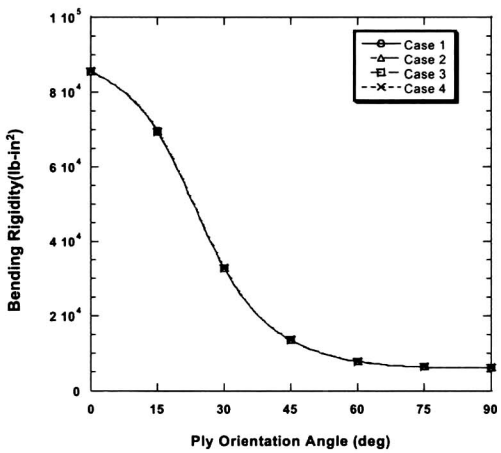

Fig. 4. Variation of bending rigidities of single-cell box beams with ply angle changes.

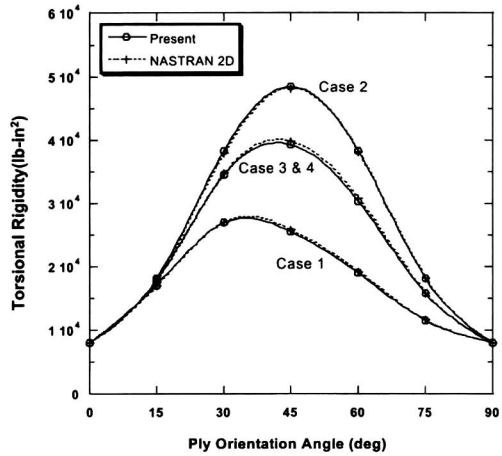

Fig. 5. Variation of torsional rigidities for single-cell box-beams with ply angle changes.

the hoop moment M_{ss} and the shear strain γ_{xs}. Fig. 4 shows the variation of the effective bending rigidity (EI_y) as a function of fiber angles of the blade. It is seen that the bending rigidities obtained for all the cases considered lead to essentially the same result. This is due to the fact that each wall has a balanced layup and there is no coupling between the membrane strains ε_{xx} and γ_{xs}. But, the existence of the coupling B_{26} is seen to influence significantly on the magnitude of torsional rigidity for the box beams. Fig. 5 shows the comparison of torsional rigidities calculated respectively for the four box-beam cases. Results obtained using the MSC/NASTRAN are also included for comparison. For the MSC/NASTRAN results, 360 CQUAD4 finite elements are used. The present results show good correlations with the MSC/NASTRAN results. Volovoi and Hodges[2] also obtained similar results for cases 2 and 3 by using their asymptotic beam model. It is seen that the elastic couplings introduced by the non-zero ply angles of box-beam walls are captured accurately in the framework of the present method.

Two-cell Rotor Blades

Numerical simulations are carried out for coupled composite blades with two-cell airfoil section. Figure 2 shows the schematic of the two-cell blade section fabricated and tested by

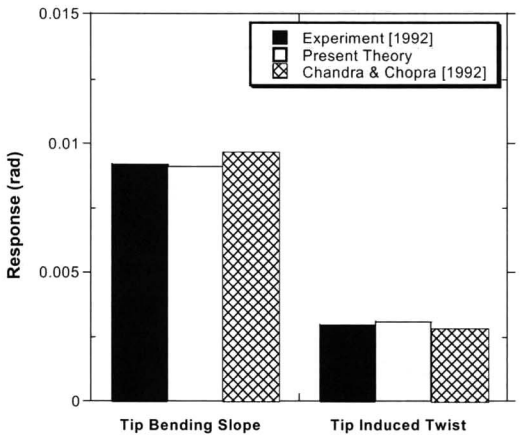

Fig. 6. Comparison of response for bending-torsion coupled blades (Blade 1) under unit tip bending load.

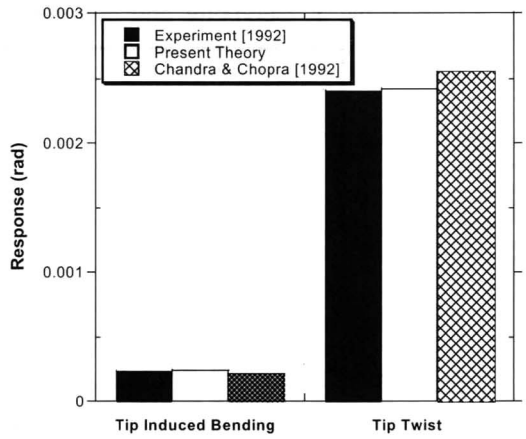

Fig. 7. Comparison of response for bending-torsion coupled blades (Blade 1) under unit tip torque load.

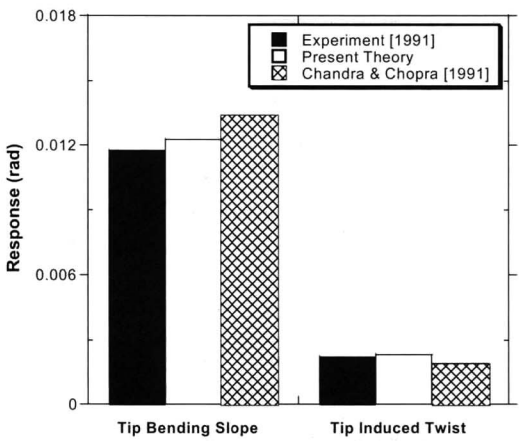

Fig. 8. Comparison of response for bending-torsion coupled blades (Blade 2) under unit tip bending load.

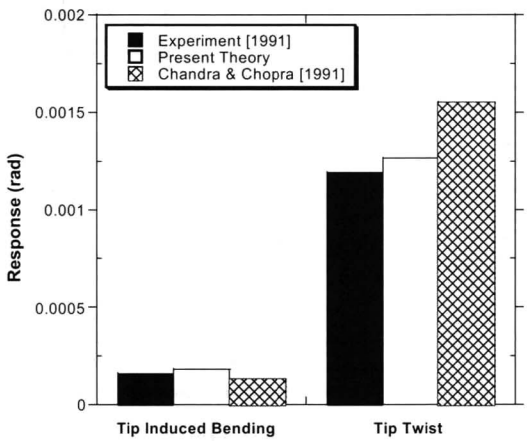

Fig. 9. Comparison of response for bending-torsion coupled blades (Blade 2) under unit tip torque load.

Table 2. Geometry and material properties of composite blades.

Properties	Values
E_{11}	131GPa
E_{22}	9.3GPa
G_{12}	5.86GPa
ν_{12}	0.40
Ply thickness	0.127mm
Airfoil	NACA 0012
Length	641.4mm
Chord	76.2mm
Airfoil thickness	9.144mm

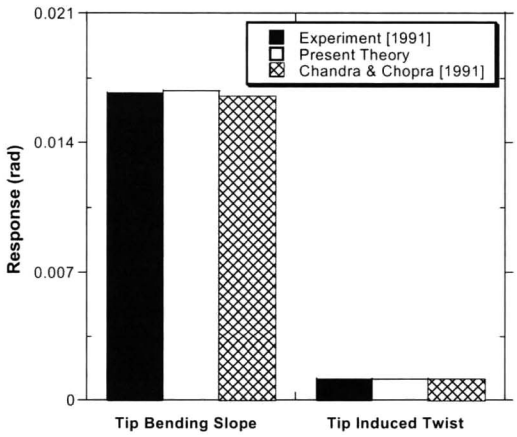

Fig. 10. Comparison of response for bending-torsion coupled blades (Blade 3) under unit tip bending load.

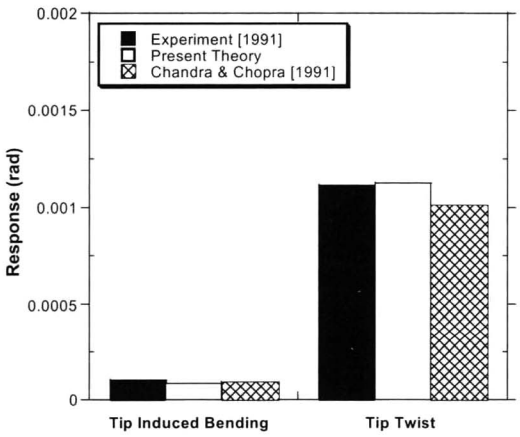

Fig. 11. Comparison of response for bending-torsion coupled blades (Blade 3) under unit tip torque load.

Table 3. Lay-up cases of bending-torsion coupled composite blades.

Case	Spar		Web	Skin
	Top Flange	Bottom Flange		
Blade 1	$[0/15]_4$	$[0/-15]_4$	$[0/\pm 15/0]_2$	[15/-15]
Blade 2	$[0/30]_4$	$[0/-30]_4$	$[0/\pm 30/0]_2$	[30/-30]
Blade 3	$[0/45]_4$	$[0/-45]_4$	$[0/\pm 45/0]_2$	[45/-45]

Chandra and Chopra[4]. The blades are clamped at one end and warping restrained at either end. The geometry and the material properties of the blades are given in Table 2. Blades with three different ply layups representing bending-torsion couplings are studied. Table 3 shows the details of the layup used in the blades.

Figure 6 shows the comparison results for the tip bending slope and induced tip twist of the bending-torsion coupled blade (Blade 1) under unit tip bending load. As is given in Table 3, Blade 1 consists of 15° spar and ±15° skin. The present results are compared with the experimental test data as well as the theoretical results obtained by Chandra and Chopra[7]. As can be seen in Fig. 6, the predictions of the present method are in good agreement with experimental results. The responses obtained by the present method are within 4.5% of the test results. The difference between the current predictions and Ref. 7 is due mainly to the fact that Chandra and Chopra[7] used the zero-in-plane strain assumption ($\gamma_{ss}=\varkappa_{ss}=0$) for the constitutive relations, while in the present approach, the zero hoop stress flow assumption ($N_{ss}=0$) is used. Figure 7 presents the tip twist and induced bending slope for Blade 1 under unit tip torsional load. There is a good correlation between the present theory and experimental results.

Figures 8 and 9 show the structural responses of the 30° blade (Blade 2) under unit tip bending and torsional loads, respectively. The present predictions are seen to be in a good agreement with experimental results. The error is within 7% of the test results. The results obtained by the present mixed method show better correlations with the experimental results than those obtained by the stiffness method of Chandra and Chopra[4]. Figures 10 and 11 show results of Blade 3 which has ply angles of 45 degrees. For this blade also, the predicted responses are within 5% of the experimental results. Note the increase in bending slope (over 30%) and decrease in induced twist (over 50%) for this blade compared with the previous blades (Blade 1 and 2).

The decrease in bending stiffness with respect to the increase in ply angles causes this aspect. The existence of bending-torsion couplings reduces the direct bending stiffness in some degree.

Concluding Remarks

In the present work, a closed-form formulation for coupled composite blades with multiple cell sections has been developed. The beam force-displacement relations of the blade were obtained by using the Reissner's semi-complementary energy functional. The resulting (7×7) stiffness matrix idealizes the blade at a Timoshenko level of approximation for bending and shear and Vlasov for torsion. It is shown that the elements of the stiffness matrix are modified by the shear related terms and shear correction terms. The theory has been correlated with experimental test data and detailed finite element results for coupled composite beams and blades with single-cell box-sections and two-cell airfoils. Good correlation of responses with experimental results was obtained for all the test cases considered. The error is less than 7% for bending-torsion coupled blades.

Acknowledgement

This work was supported in part by research funds of Chonbuk National University. The research was performed for the Smart UAV Development program, one of 21st Century Frontier R&D Programs funded by the Ministry of Science and Technology of Korea.

References

1. Mansfield, E. H., "The Stiffness of a Two-Cell Anisotropic Tube," *Aeronautical Quarterly*, May 1981, pp. 338-353.

2. Volovoi, V. V., and Hodges, D. H., "Single- and Double-Celled Composite Thin-Walled Beams," *Proceedings of the 41st Structures, Structural Dynamics, and Materials Conference*, Atlanta, GA, Apr. 3-6, 2000, AIAA Paper 2000-1537.

3. Badir, A. M, "Analysis of Two-Cell Composite Beams," *Proceedings of the 36th Structures, Structural Dynamics, and Materials Conference*, New Orleans, LA, Apr. 10-12, 1995, pp. 419-424.

4. Chandra, R., and Chopra, I., "Coupled Composite Rotor Blades under Bending and Torsional Loads," *AHS Specialists Meeting on Rotorcraft Structures*, Williamsburg, Virginia, Oct. 28-31, 1991.

5. Jung, S. N., Nagaraj, V. T., and Chopra, I., "Refined Structural Model for Thin- and Thick-Walled Composite Rotor Blades," *AIAA Journal*, Vol. 40, No. 1, Jan. 2002, pp. 105-116.

6. Gjelsvik, A., *The Theory of Thin Walled Bars*, John Wiley & Sons, Inc., 1981.

7. Chandra, R., and Chopra, I., "Structural Response of Composite Beams and Blades with Elastic Couplings," *Composites Engineering*, Vol. 2, Nos. 5-7, 1992, pp. 347-374.